

Fabrication of a Simple and Sensitive Electrochemical Dicyandiamide Sensor Based on Molecularly Imprinted Technology

Hongwu Wang^{*}, Yanqing Liu^{*}, Shoulian Wei, Su Yao, Siyi Gong

School of Chemistry and Chemical Engineering, Zhaoqing University, Zhaoqing, 526061, China

*E-mail: hwwangcn@hotmail.com, yqliucn@hotmail.com

Received: 12 August 2015 / Accepted: 10 September 2015 / Published: 30 September 2015

A novel electrochemical sensor for dicyandiamide (DCD) recognition and detection was fabricated by using molecularly imprinted polymer (MIP) technique. The MIP sensor was electropolymerized on the surface of a golden electrode via cyclic voltammetry (CV). The properties of the MIP sensor were characterized via CV and differential pulse voltammetry (DPV) by using potassium ferricyanide/potassium ferrocyanide as an electroactive probe. The results showed that the response peak current was linearly related with DCD concentrations from 0.01 $\mu\text{mol/L}$ to 4 $\mu\text{mol L}^{-1}$ and a limit of detection of 0.3 nmol L^{-1} (S/N = 3). The sensor was satisfactorily employed to monitor the infant formula.

Keywords: Dicyandiamide; Electrochemical sensor; Molecularly Imprinted Polymer; Infant formula

1. INTRODUCTION

Dicyandiamide (DCD) or cyanoguanidine is a dipolymer of cyanamide produced in large scale from nitro-chalk through the intermediate compound cyanamide. DCD is widely used as a nitrification inhibitor to hinder the activity of nitrifying bacteria in agriculture and consequently reduce the rates of nitrification and nitrogen loss in soil [1-3]. However, the widespread use of DCD can result in DCD residues on pastures, causing threat to human health, particularly in infants through baby formulas. Studies have detected DCD in infant formulas. Given the high nitrogen content of DCD, unscrupulous traders may add DCD to milk samples to increase the nitrogen content. Hence, a fast, sensitive, and accurate method is desirable to measure the residue levels of DCD in infant formulas.

Various methods, such as UV spectroscopy [4], Raman chemical imaging [5], ion-exclusion chromatography [6], high performance liquid chromatography (HPLC) [7], electrospray ionization

mass spectrometry (ESI–MS) [8], and liquid chromatography–tandem mass spectrometry (LC–MS)[9–11] have been developed for the detection of DCD in milk. However, it was difficult to employ because it usually need sophisticated equipment, and the operator should be professional. In most cases, these methods require complicated sample preparations, including extraction, preconcentration, and derivatization, etc [10,11].

Molecular imprinting is a very promising technology for preparing polymer with specific recognition sites [12]. Such polymer has specific bonding effects to specific target molecules [13]. Compared with natural biological receptors, molecularly imprinted polymers (MIPs) provide unique advantages of physical and chemical stabilities, strong affinities, excellent substrate recognition, low cost, and easy preparation [14–22]. MIPs have been satisfactorily applied in different fields including chromatography [23–26], solid-phase extraction [27–29], and chiral separation [30–32]. Moreover, MIPs are widely accepted as molecular recognition materials for chemical sensors [33–38].

To our knowledge, MIP electrochemical DCD sensor was rarely reported. In the present study, we report a simple, rapid, selective, and efficient quantitative approach to detect DCD residues through modification of a DCD-imprinted polymer film onto a golden electrode.

2. EXPERIMENTAL

2.1. Reagents and instruments

DCD was bought from Sigma-Aldrich Co. (St. Louis, MO, USA). *o*-Aminophenol (*o*-AP) was obtained from Kemiou Chemical Reagent Co., Ltd. (Tianjin, China). Potassium hexacyanoferrate ($K_3[Fe(CN)_6]$) and potassium ferrocyanide ($K_4[Fe(CN)_6]$) were purchased from Sinopharm Group Chemical Reagent Co., Ltd.

Unless otherwise indicated, the used reagents were of analytical grade. Double-distilled water was used throughout the experiments. The CHI660E electrochemical workstation was obtained from Chenhua Instrument Co., Ltd. (Shanghai, China). Electrochemical data were performed with a three-electrode system. The golden electrode (GE) ($\Phi = 2$ mm), a platinum wire electrode and an Ag/AgCl electrode were employed as a working, auxiliary, and reference electrode, respectively.

2.3 Preparation of MIP-modified electrodes

After polished with 0.05 μm slurry of alumina powder, the GE was sonicated in double-distilled water for 5 min. The polished electrodes were activated in 0.5 mol L⁻¹ H₂SO₄ by cyclic voltammetry (CV) from -0.20 to 1.60 V under the scan rate of 100 mV/s until the reproducible voltammograms were gotten.

MIP electropolymerization was constructed in a solution containing 0.10 mmol L⁻¹ DCD and 5 mmol L⁻¹ *o*-AP and 0.2 mol L⁻¹ Na₂HPO₄-NaH₂PO₄ buffer solutions (pH = 5.8). The potential was set at the range of -0.3 V to 1.2 V at 50 mV S⁻¹ for 10 cycles.

Non-imprinted polymer (NIP) electrode was prepared under the same conditions in the absence of DCD.

2.4 Sample preparation

Before analyzing the sample, 10 mL of milk was added to an equal solution of ethanol. The mixture was centrifuged at 15000 rpm. The supernatant was collected and then filtered through a 0.45 μm membrane to eliminate the interference measurement of protein adsorption on the surface of the membrane electrode.

3. RESULTS AND DISCUSSION

3.1 DCD polymerization

The CV for *o*-AP electropolymerization in the presence of DCD on the surface of the GE indicates the anodic peak at 0.632 V potential (E_p) and $-31.58 \mu\text{A}$ current (i_p). The curve shape shows that the *o*-AP electrochemical polymerization on the GE is a totally irreversible process. The current density decreased when the number of CV increased, thereby forming a dense non-conductive film. The film gradually covered the electrode surface, resulting in voltammetric response inhibition.

The CV for the NIP electropolymerization was roughly similar to that of MIP, indicating that no electrochemical activities of DCD occurred during the polymerization process (-0.3 V to 1.2 V) when the GE was performed as the working electrode and sulfuric acid as the bottom liquid. Thus, no electrochemical change was observed on the structure of the template molecule while the polymer was in DCD.

3.2 Structure of molecularly imprinted films

Uniform and dense *o*-AP membranes with open structures can be synthesized by *o*-AP electropolymerization in acidic solution condition.

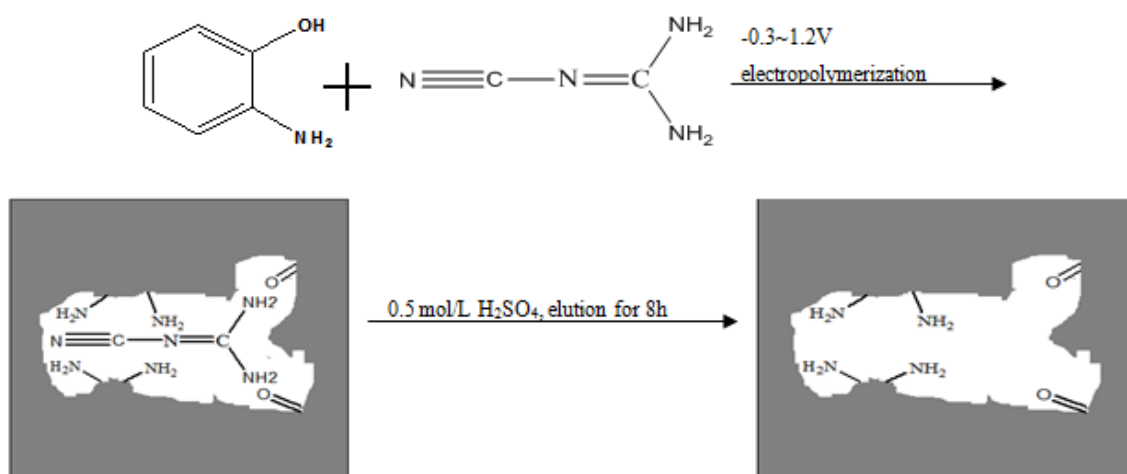


Figure 1. the formation process of DCD molecularly imprinted polymer

Given that the main form of DCD is DCDH^+ [39–40], the existence of hydrogen bond in the molecularly imprinted films under pH 4.5 can be inferred. The recognition sites (hydrogen bonding) in the imprinted membrane were destroyed when the DCD template molecules were rinsed with 0.5 mol/L sulfuric acid solution, bringing out the molecules escaping from the 3D cavities of the molecularly imprinted membrane. The formation process of DCD MIP is shown in Figure 1. DCD molecules can enter the molecularly imprinted membrane by hydrogen bonding in $0.01 \text{ mol L}^{-1} \text{ K}_3[\text{Fe}(\text{CN})_6]$ testing solution, thereby producing the sensor response.

3.3 Characterization of MIP film

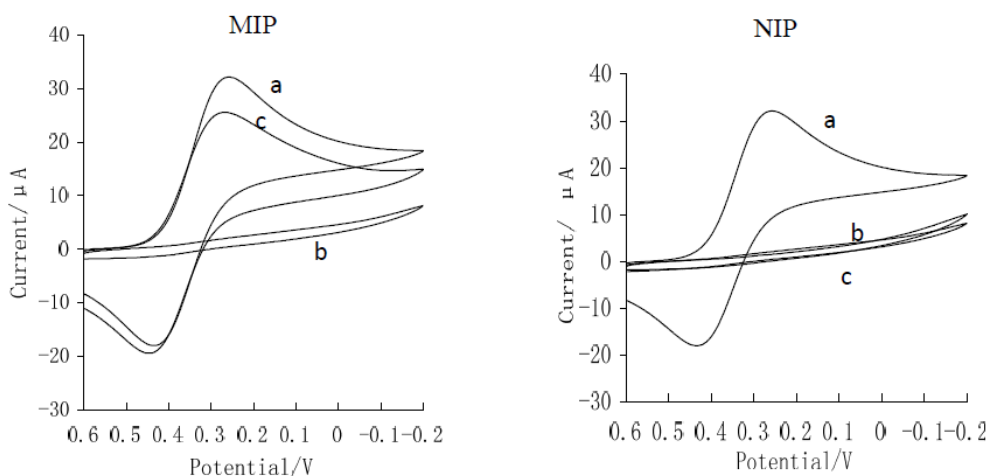


Figure 2. CV of (a) Bare electrode, (b) after electropolymerization, and (c) after removing template in $5 \text{ mmol L}^{-1} \text{ K}_3[\text{Fe}(\text{CN})_6]$ solution

The DPV was applied for the characterization of the polymer film. On the basis of the signal change in the oxidation current for potassium ferricyanide and the reduction current for ferrocyanide, the morphology and characteristics of the polymer film were studied using $\text{K}_3[\text{Fe}(\text{CN})_6]$ as the electrochemical probe because the membrane cavities on the surface of the disc electrode can be used as electron-transfer channels.

The CVs of DCD MIP and NIP in $5 \text{ mmol L}^{-1} \text{ K}_3[\text{Fe}(\text{CN})_6]$ solution are shown in Figure 2. For the MIP membrane electrode, the CV curve is parallel, and the redox peaks of the electrode surface almost cannot be observed. The results illustrated that the redox reactions between the bottom liquid and the surface of the GE were hindered because the existing dense was imprinted poly *o*-AP film. The peak current density increased because $[\text{Fe}(\text{CN})_6]^{3-}$ ions reacted at the GE by diffusing to the imprinted cavities that appeared after elution.

However, for the NIP film electrode, probe protons cannot react by penetrating the polymer membrane. The dense non-imprinted form of poly *o*-AP film existed at the bare GE surface. No peak was observed, and the CV curves of MIP and NIP were almost the same. The cleaning of NIP film can only remove small amounts of *o*-AP monomer, which did not participate in the polymerization process, thereby causing no molecular imprinting cavities on the polymer membrane after elution.

Therefore, the NIP film did not generate an ion-transfer channel because the density of the NIP film was higher than the MIP. The experiments indicated that the DCD recognition sites were existed in the molecularly imprinted membrane.

3.4 Molecular imprinting effect

Under $0.01 \text{ mmol L}^{-1} \text{ K}_3[\text{Fe}(\text{CN})_6]$, the electrochemical reduction reaction of $[\text{Fe}(\text{CN})_6]^{3-}$ ion occurred on the surface of the bare GE with the peak current at $28.79 \mu\text{A}$ potential. Almost no electrochemical reaction was observed at the MIP electrode before template removal and at the NIP electrode after washing. The poly *o*-AP film demonstrated poor conductivity, and the GE surface binding was closed. Electrochemical reaction was observed on the surface of the MIP electrode after washing with 0.5 mol L^{-1} sulfuric acid with a peak current that significantly decreased at $19.17 \mu\text{A}$ potential, which suggested that the $[\text{Fe}(\text{CN})_6]^{3-}$ ion electrochemical reaction occurred on the surface of the GE by going through the imprinted membrane with 3D imprinting “hole” after template removal. However, the area of the bare electrode relatively decreased. This result further proved the existence of a molecularly imprinted membrane.

3.5. Experimental parameters optimization

In order to achieve the optimal operation of the MIP sensor, several parameters, such as electropolymerization scan cycles, molar ratios of template molecules to functional monomers, extraction time, and incubation time on the current response, were investigated.

3.5.1 Optimization of electropolymerization scan cycles

Membrane thickness directly affects the sensitivity and selectivity of MIP sensors. To investigate the effects of electropolymerization scan cycles, the membranes were prepared and investigated using a series of scan cycles of 8, 12, 16, 20, and 24 during the electropolymerization process. As shown in Figure 3A, the current response gradually increased when the scan cycles increased and reached the maximum at 16 cycles. After 16 cycles, the current response decreased when the scan cycles increased, indicating that the membranes were thick and cannot completely remove the template molecules. After electropolymerized 20 cycles, the membrane can achieve the highest selectivity and sensitivity to DCD.

3.5.2. Effect of molar ratios of template molecules to functional monomers

To investigate the effects of different molar ratios of template molecules to functional monomers on the current, a series of membranes was prepared and investigated using different molar ratios. When the molar ratio was set at 2:3, the MIP sensor showed the strongest current signal (Figure 3B). At lower molar ratio, the current signals notably decreased, probably because excessive amount of

functional monomers prevented the targets close to the electrode surface. At higher molar ratio, the current response also notably decreased, possibly because the functional monomers were insufficient to combine with the excess of template molecules, thereby decreasing the number of available recognition sites. As a result, the optimal molar ratio was set at 2:3 in the current work.

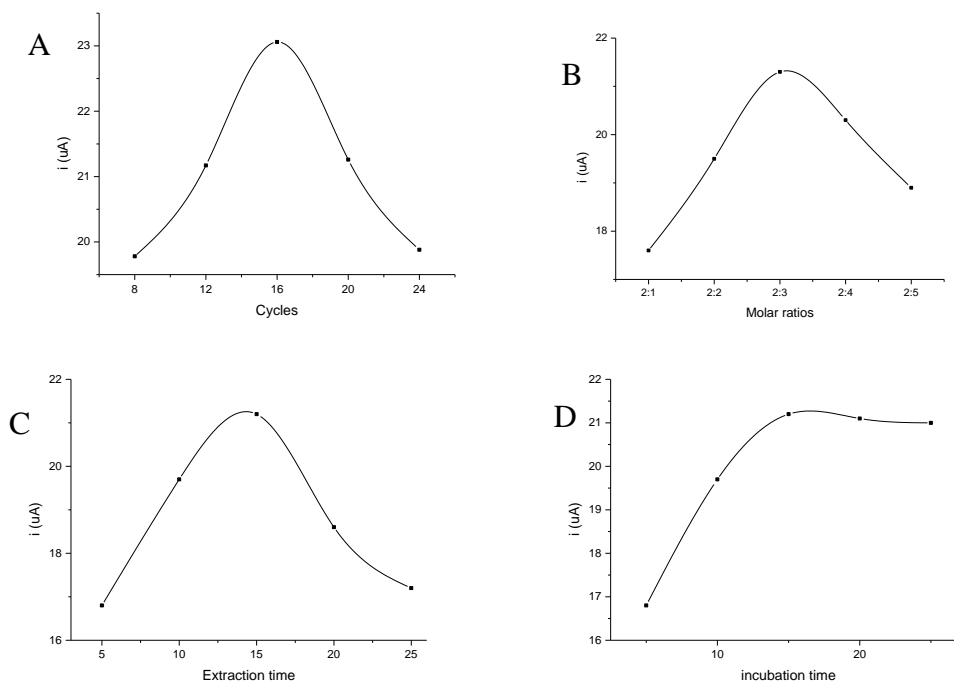


Figure 3. A: Effects of the cycles B: Effects of the molar ratios C: Effects of the extraction time D: Effects of the incubation time

3.5.3. Influence of extraction time

In order to investigate the effect of extraction time on the current signals and remove the template molecules, the prepared sensors were washed in hydrochloric acid solution (0.1 mol L^{-1}) for 5, 10, 15, 20, and 25 min at room temperature (RT). As shown in Figure 3C, the current response enhanced when the extraction time prolonged and reached the maximum at 15 min. After 15 min, the current signals decreased, suggesting that 15 min duration is adequate to remove the template molecules.

3.5.4. Influence of incubation time

MIP sensors were incubated in DCD solution for 5, 10, 15, 20, and 25 min at RT to optimize the incubation time and thus improve the recognition ability of the sensor. As shown in Figure 3D, with prolonged incubation time, the current response gradually strengthened, and achieved balance at 10 minutes. It declared that the adsorption equilibrium was achieved. Hence, the incubation time of imprinted sensor was set at 15 minutes.

3.6 Linear range and limit of detection

The MIP sensor was rinsed in double-distilled water and then placed in $0 \mu\text{mol L}^{-1}$ to $30 \mu\text{mol L}^{-1}$ DCD for 12 min. The DPV responses of the MIP sensor in $5 \text{ mmol K}_3[\text{Fe}(\text{CN})_6]$ solution are shown in Figure 4. The sensor was sonicated in 0.5 mol L^{-1} sulfuric acid after each determination to elute the template molecules. The curve of the sensor after eluted the template is shown in curve 1, and the curves of 2 to 14 with the corresponding peak current of MIP membrane electrode immersed in the concentration of DCD standard solution were studied. As shown in Figure 4A, the peak current rapidly lowered when the template concentration increased. It suggested that with increase of adsorbed template molecules, more imprinted cavities were closed and mass-transfer diffusion was blocked. The linear regression equation and the correlation coefficient (R^2) were expressed as $y = 1.7531x + 10.645$ ($R^2 = 0.9948$), where y and x are the peak current reduction (μA) of hexacyanoferrate and the concentration of DCD ($\mu\text{mol L}^{-1}$), respectively (see Figure 4B). The linear response range of the imprinted sensor was $0.01 \mu\text{mol L}^{-1}$ to $4 \mu\text{mol L}^{-1}$ for DCD with the detection limit of 0.3 nmol L^{-1} or 0.025 ng mL^{-1} .

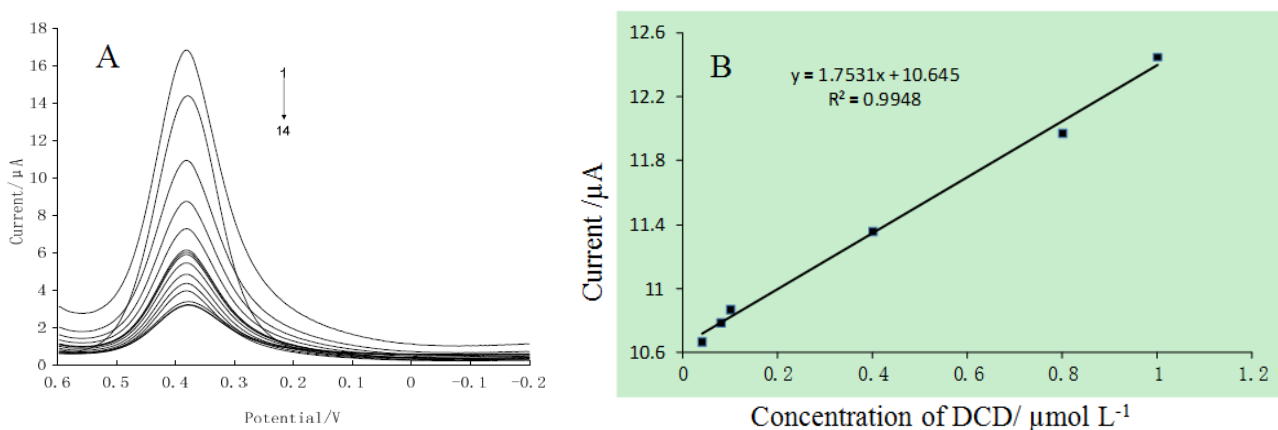


Figure 4. A: DPV responses of the MIP sensors at $0 \mu\text{mol L}^{-1}$ to $30 \mu\text{mol L}^{-1}$ DCD. B: The linear relationship between the peak current and the concentration of DCD

3.7 Reproducibility and stability

The used MIP electrode was eluted twice for 20 min, and the determined response value was consistent with the original one. The sensor was parallel tested for six times in 1.0 nmol L^{-1} of DCD. The current response RSD was 1.8%, which demonstrated good reproducibility of the imprinted sensor. The sensor initial response decreased by 85% after being used repeatedly for ten times, probably because the structure of the imprinted cavities was gradually destroyed during the process of repeated elution and adsorption on membrane electrode. The recognition sites lost the binding capacity to the DCD molecules.

3.8 Real sample analysis

The MIP sensor was employed to measure the DCD content in infant formula samples. The results are summarized in Table 1.

Table 1. Average recovery and relative standard deviation of DCD ($n = 3$)

Added concentration (nmol L ⁻¹)	Detected concentration (nmol L ⁻¹)	Recovery (%)	RSD (%)
50	48.6	97.2	3.57
100	98.7	98.7	2.38
500	488.7	97.7	1.65
1000	978.7	97.9	2.67

The recoveries for infant formula samples varied from 97.2% to 98.7% with RSD of <3.57%. Furthermore, the recent methods for monitoring dicyandiamide in milk samples were summarized in Table 2. It was shown that the LODs of the proposed MIP sensor method were lower than those of FI-CL[41], Colorimetric sensing [42] and UPLC-ESI-MS/MS[43]. Therefore, the proposed MIP sensor was a simple, suitable and sensitive electrochemical sensor for monitoring DCD in infant formula samples.

Table 2. Comparison of the proposed method with other methods

Analytical method	LOD (ng mL ⁻¹)	Recoveries (%)	RSD (%)	References
FI-CL	3.0	87.0–102.3	1.2–2.9	41
Colorimetric sensing	6.7	94–109		42
UPLC-ESI-MS/MS	1	83.7–96.7	1.1–1.8	43
SID-HILIC-MS/MS	0.01	110.8	7.4	44
MIP sensor	0.025	97.2–98.7	1.65–3.57	This work

4. CONCLUSION

In this work, we developed a simple, suitable and sensitive molecularly-imprinted electrochemical sensor for the monitoring DCD. The MIP films were electropolymerized on the surface of the GE. The preparation conditions of the sensor, such as electropolymerization scan cycles, molar ratios of template molecules to functional monomers, extraction time, and incubation time on the current response, were investigated and discussed. The proposed MIP sensor possessed outstanding performance such as a low LOD, high sensitivity toward DCD. It was satisfactorily employed to measure DCD in real samples.

ACKNOWLEDGEMENTS

This work was supported by the Major Projects of Department of Education of Guangdong Province (2014KZDXM074), the Project of Department of Education of Guangdong Province (2013KJCX0191, 2014KTSCX193), the Special Projects of Higher Education Talent Introduction of Guangdong Province (2013197), the Project of Science and Technology Planning of Zhaoqing City (2013F013), the Science and Technology Planning Project of Zhaoqing High-technology Zone (2012B01003002) and the Science and Technology Planning Project of Zhaoqing University (201318).

References

1. H.J. Di, K.C. Cameron, J.P. Shen, C.S. Winefield, M. O'Callaghan, S. Bowatte and J. Z. He, *Nat. Geosci.*, 2 (2009) 621.
2. T. Lan, Y. Han, M. Roelcke, R. Nieder and Z. Cai, *Soil Biol. Biochem.*, 67 (2013) 174.
3. C. Schwarzer and K. Haselwandter, *J. Chromatogr. A*, 732 (1996) 390.
4. H. Zou, W. Zhang and Y. Feng and B. Liang, *Anal. Method*, 6 (2014) 5865.
5. J. Qin, K. Chao, M.S. Kim, *Food Chem.*, 138 (2013) 998.
6. M. Chen, G. Pan and K. Dai, X. Zeng and M. Ye, *Chinese J. Anal. Chem.*, 41 (2013), 1734.
7. Y. Nagumo, K. Tanaka, K. Tewari, K. Thiraporn, T. Tsuchida, T. Honma, N. Ohtake, K. Sueyoshi, Y. Takahashi, T. Ohyama, *J. Chromatogr. A*, 1216 (2009) 5614.
8. J. Cummins, J. Hull, K. Kitts, and J.V. Goodpaster, *Anal. Method*, 3 (2011) 1682.
9. G. Abernethy and K. Higgs, *J. Chromatogr. A*, 1288 (2013) 10.
10. X. Chen, L. Zhou, Y. Zhao, S. Pan and M. Jin, *Talanta*, 149 (2014) 187.
11. Y. Shen, C. Han, X. Zhou, F. Huang and Z. Zhu, *J. Dairy Sci.*, 96 (2013) 6877.
12. K. Mosbach. *Trends Biochem. Sci.*, 19 (1994) 9.
13. T. Takeuchi and J. Haginaka, *J. Chromatogr. B*, 728 (1999) 1.
14. C. Baggiani, C. Giovannoli, L. Anfossi, C. Passini, P. Baravalle and G. Giraudig. *J. Am. Chem. Soc.*, 134 (2012) 1513.
15. S. Banerjee and B. Koenig, *J. Am. Chem. Soc.*, 135 (2013) 2967.
16. D. Cai, L. Ren, H. Zhao, C. Xu, L. Zhang, Y. Yu, H. Wang, Y. Lan, M. F. Roberts, J.H. Chuang, M. J. Naughton, Z. Ren and T. C. Chiles *Nat. Nanotechnol.*, 5 (2010) 597.
17. X. Que, B. Liu, L. Fu, J. Zhuang, G. Chen and D. Tang, *Electroanal.*, 25 (2013) 531.
18. P.S. Sharma, F. D'Souza and W. Kutner, *TRAC-Trend. Anal. Chem.*, 34 (2012) 59.
19. X. Shen, L. Zhu, C. Huang, H. Tang, Z. Yu and F. Deng. *J. Mater. Chem.*, 19 (2009) 4843.
20. C. Xie, H. Li, S. Li, J. Wu and Z. Zhang, *Anal. Chem.*, 82 (2010) 241.
21. A. Yarman and F.W. Scheller, *Angew. Chem. Int. Edit.*, 52 (2013) 11521.
22. M. Zhao, C. Zhang and Y. Zhang, X.Guo, H. Yan and H. Zhang, *Chem. Commun.*, 50 (2014) 2208.
23. F. Ahmadi, H. Rezaei and R. Tahvilian, *J. Chromatogr. A*, 1270 (2012) 9.
24. H. Ebrahimzadeh, K. Molaei, A.A. Asgharinezhad, N. Shekari and Z. Dehghani. *Anal. Chim. Acta*, 767 (2013) 155.
25. J.M. Lerma-García, M. Zougagh and A. Ríos, *Microchim. Acta*, 180 (2013) 363.
26. J.L. Urraca, M. Castellari and C.A. Barrios, and M.C. Moreno-Bondi, *J. Chromatogr. A*, 1343 (2014) 1.
27. EA. Mbukwa, T.A.M. Msagati and B.B. Mamba, *Anal. Bioanal. Chem.*, 405 (2013) 4253.
28. H. Sun, J. Lai and Y. Fung, *J. Chromatogr. A*, 1358 (2014) 303.
29. Y. Wang, E. Wang and Z. Wu, H. Li, Z. Zhu, X. Zhu and Y. Dong, *Carbohydr. Polym.*, 101 (2014) 517.
30. R.J. Ansell, J.K.L. Kuah and D. Wang, C.E. Jackson, K.D. Bartle and A.A. Clifford, *J. Chromatogr. A*, 1264 (2012) 117.
31. B. Huang, Y. Chen, G. Wang and C. Liu, *J. Chromatogr. A*, 1218 (2011) 849.

32. X.N. Wang, R.P. Liang, X.Y. Meng and J.D. Qiu, *J. Chromatogr. A*, 1362 (2014) 301.
33. T.H. Bui, M. Seo and X. Zhang, X.Zhang and Y.I. Lee, *Biosens. Bioelectron.*, 57 (2014) 310.
34. Y. Fuchs O. Soppera, A.G. Mayes and K. Haupt, *Adv. Mater.*, 25 (2013) 566.
35. Y. Mao Y. Bao, S. Gan, F. Li and L. Niu. *Biosens. Bioelectron.*, 28 (2011) 291.
36. H. Qiu C. Luo, M. Sun, F.Lu,L.Fan and X.Li *Anal. Chim. Acta*, 744 (2012) 75.
37. P.S. Sharma A. Pietrzyk-Le, F. D'Souza and W. Kutner. *Anal. Bioanal. Chem.*, 402 (2012) 3177.
38. G. Yao, R. Liang, C. Huang, Y.Wang and J.-D.Qiu *Anal. Chem.*, 85 (2013) 11944.
39. M. Peeters, F.J. Troost, R.H.G. Mingels, T. Welsch, B. van Grinsven, T. Vranken, S. Ingebrandt, R. Thoelen, T.J. Cleij and P. Wagner, *Anal. Chem.*, 85 (2013) 1475.
40. A. Zhang Y. Chen and Z. Tian, *Acta Phys.-Chim. Sin.*, 4 (1991) 146.
41. H. Yu, Y.Tang, G. Zhang, Z. Wang and R. Gao, *J. Lumin.*, 157 (2015) 327.
42. J. Liu, X. Zhang, C. Xiao, A. Yang, H. Zhao, Y. He, X. Li and Z. Yuan, *Microchim. Acta*, 182 (2015) 435.
43. F. Feng, P. Jiang, N. Li, H. Zhou and X. Chu. *Chinese J. Anal. Chem.*, 41 (2013) 1729.
44. K. Inoue, T. Sakamoto, J. Min, K. Todoroki and T. Toyo'oka, *Food Chem.*, 156 (2014) 390.

© 2015 The Authors. Published by ESG (www.electrochemsci.org). This article is an open access article distributed under the terms and conditions of the Creative Commons Attribution license (<http://creativecommons.org/licenses/by/4.0/>).